

# A new consistent and high-precision earthquake catalogue for the Taupō Volcanic Zone, New Zealand

Finnigan Illsley-Kemp \*<sup>1</sup>, Eleanor R. H. Mestel <sup>1</sup>

<sup>1</sup>School of Geography, Environment and Earth Science, Victoria University of Wellington, New Zealand

**Author contributions:** *Conceptualization:* Finnigan Illsley-Kemp. *Methodology:* Finnigan Illsley-Kemp, Eleanor R. H. Mestel. *Formal Analysis:* Finnigan Illsley-Kemp, Eleanor R. H. Mestel. *Writing - Original draft:* Finnigan Illsley-Kemp. *Writing - Review & Editing:* Finnigan Illsley-Kemp, Eleanor R. H. Mestel. *Funding acquisition:* Finnigan Illsley-Kemp.

**Abstract** The Taupō Volcanic Zone is a ~300 km long, volcanically active region in the North Island of Aotearoa New Zealand. As well as hosting numerous active volcanoes, it is also one of the most seismically active parts of the country. In this study, we present a new consistent and high-precision earthquake catalogue for the Taupō Volcanic Zone from 2007 to 2023. This catalogue was produced through the detection of earthquake phase arrivals, association of these arrivals, and finally earthquake location and relocation using a three-dimensional velocity model. The final catalogue contains 86,579 individual earthquakes, 65% of which also have a high-precision relative relocation hypocentre. The catalogue contains a huge amount of information on multiple volcanic, geothermal, and tectonic events. We make the catalogue freely available in the hope that it will be used for future research and development in the Taupō Volcanic Zone.

Production Editor:  
Gareth Funning  
Handling Editor:  
Lise Retailleau  
Copy & Layout Editor:  
Anant Hariharan

Signed reviewer(s):  
Aude Lavayssière,  
Daniel Trugman

Received:  
October 16, 2024  
Accepted:  
March 31, 2025  
Published:  
May 2, 2025

## 1 Introduction

The Taupō Volcanic Zone (TVZ, Figure 1a) is one of the most seismically active regions of Aotearoa New Zealand. Much of this seismicity is small in magnitude, and related to the numerous volcanic and geothermal systems in the TVZ (e.g., Hurst et al., 2008; Hopp et al., 2019; Illsley-Kemp et al., 2022). However, the TVZ also hosts an active continental rift (Seebeck et al., 2014) and is capable of producing large earthquakes (e.g., the 1987  $M_w$  6.5 Edgecumbe earthquake, Smith and Oppenheimer, 1989; Delano et al., 2022). Earthquake activity in the TVZ, and in New Zealand as a whole, is routinely monitored by GeoNet using the national seismic network (Petersen et al., 2011; GNS Science, 2024). There have also been many individual studies of earthquake sequences in the TVZ, as well as multiple temporary seismic deployments (e.g., Webb et al., 1986; Sherburn, 1993; Sherburn et al., 1999; Bryan et al., 1999; Hayes et al., 2004; Bannister et al., 2016; Benson et al., 2021; Illsley-Kemp et al., 2021; Lamb et al., 2024). The 24/7 monitoring of earthquake activity by GeoNet is essential for hazard mitigation purposes; however, the catalogue produced is not of sufficient accuracy for many research purposes, particularly at volcanic and geothermal systems where earthquakes tend to be low magnitude. In addition, the lack of uniformity in data-processing approaches across catalogues makes it challenging to compare earthquake activity from different time-periods, something which is crucial for many purposes, such as volcano monitoring.

The purpose of our study was to develop and present a consistent and high-precision earthquake catalogue for the entirety of the TVZ from 2007–2023. Our study is limited to the crustal seismicity of the TVZ (i.e. <50 km depth) and does not consider the underlying subduction zone seismicity (e.g., Mark et al., 2024). We fully document each of the processing steps and make all of the underlying data openly available, with the hope that this catalogue can continue to be developed with the addition of newly available seismic data. We envisage that this catalogue will be used for a wide variety of research purposes in the future.

## 2 Methods

Below, we describe each distinct stage of generating the TVZ earthquake catalogue. Each stage requires choices of parameters which we selected with the aim of producing the most consistent and accurate earthquake catalogue. However, some of these choices are naturally subjective and so we detail each stage in order to make our workflow fully reproducible and adjustable for other researchers.

### 2.1 Seismic data

We used all seismic data from the TVZ that was publicly available between 2007/01/01 and 2024/01/01 (UTC). The vast bulk of this data was from the GeoNet national seismic network (GNS Science, 2019, 2021). At the beginning of 2007 this network consisted of 40 seismic

\*Corresponding author: finnigan.illsleykemp@vuw.ac.nz

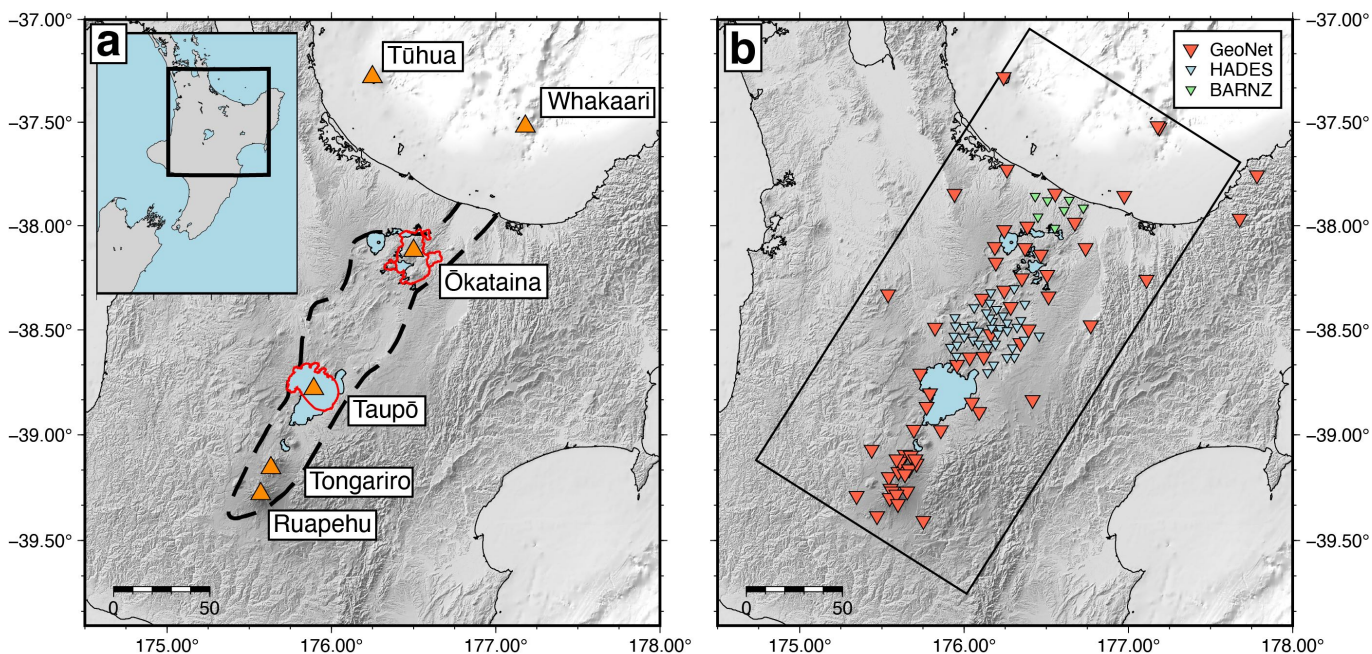


**Figure 1** a) The Taupō Volcanic Zone and its position in the North Island of New Zealand (inset). The dashed black outline denotes the approximate outline of the modern Taupō Volcanic Zone (Wilson et al., 1995, 2009). Orange triangles denote active volcanic centres with the caldera margins of Taupō and Ōkataina shown in red. b) The seismometers used in this study. The red inverted triangles denote the GeoNet National Seismic Network (as of 2023), blue and green inverted triangles denote the temporary HADES and BARNZ networks, respectively. The black outline shows the region displayed in the subsequent Figures 4, 5, and 6.

sensors, but over time this has been steadily increased to 62 sensors. The national GeoNet seismic network in the TVZ is predominantly made up of short-period seismometers, but in recent years the proportion of broadband seismometers has increased. The spacing of these seismometers is relatively consistent ( $\sim 10 - 20$  km), with the exception of Ruapehu and Tongariro volcanoes, which are more densely instrumented (Figure 1b).

During the time period 2007–2023, there were also two temporary seismic deployments whose data were publicly available at the time of data processing. The first of these was the Deep Geothermal HADES seismic array, which was active in the central TVZ between 2009–2011 and consisted of 39 broadband and short-period seismometers (Bannister, 2009), and the second was the Back-Arc Rifting in New Zealand (BARNZ) seismic array which was active in the northern TVZ between 2017–2019 and consisted of seven broadband seismometers (Ebinger and Stern, 2017). The data from these temporary deployments were integrated with the national seismic network and processed in the same way. Naturally, the temporal changes in seismic network density will mean that the earthquake detection capability will change over time.

## 2.2 Automatic picking

To generate phase-arrival picks for our data, we used the *SeisBench* (Woollam et al., 2022) implementation of *EQTransformer* (Mousavi et al., 2020). *EQTransformer* is

a machine-learning algorithm that has been trained on a global earthquake dataset (Mousavi et al., 2019). The earthquake dataset used for training is well suited to our study as the majority of earthquakes in the training dataset are shallow ( $< 50$  km), have magnitudes across a broad range ( $-0.5 - 7.9$ ), and are recorded on three-component seismic data (Mousavi et al., 2019). We applied an overlapping window of 55 seconds to account for bias in the pick probabilities (Pita-Sllim et al., 2023). We used the conservative pre-trained model from Mousavi et al. (2020), which is designed to minimise false-positives, and retained arrival-time picks where the event probability was  $\geq 0.2$  and the pick probability was  $\geq 0.01$  ( $P$  or  $S$ ). This approach tends to produce many duplicate picks so it was necessary to decluster the initial output. We first removed any complete duplicates (i.e., picks with the same time and peak probability value), and then for any picks with the same phase that were within 5 seconds of each other, the pick with the highest probability was retained. After this process, we were left with  $3.5 \times 10^7$  picks across 105 unique seismometers. The daily number of picks is almost always  $> 10^3$ , and occasionally  $> 10^4$  (Figure 2). However at this stage, prior to association, many of these picks can be attributed to large earthquakes outside of the TVZ.

## 2.3 Earthquake associating

In order to associate individual phase picks to earthquakes, we used the *PyOcto* earthquake associator (Münchmeyer, 2024). *PyOcto* is a python-based associator which divides the space and time dimensions of the problem using an OctoTree approach. In order to

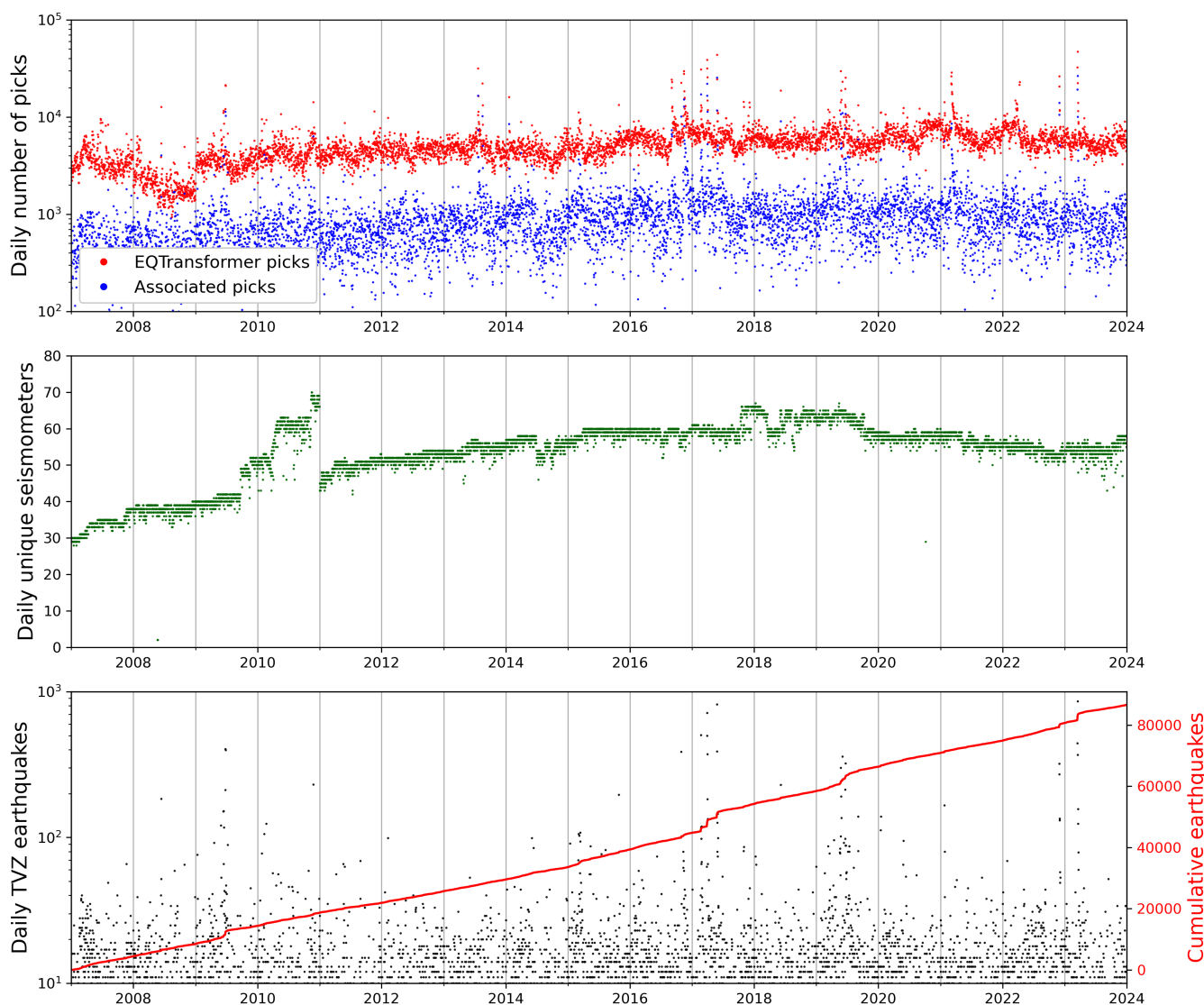


**Figure 2** a) Red denotes the daily number of picks produced by *EQTransformer* (Mousavi et al., 2020) across all seismometers. Blue denotes the daily number of these picks that were associated by *PyOcto* (Münchmeyer, 2024) to earthquakes in the TVZ. b) Green denotes the daily number of seismometers that had at least one pick. This shows the steady increase in GeoNet sensors from 2007, and the temporary deployments between 2009–2011 and 2017–2019 (Bannister, 2009; Ebinger and Stern, 2017). c) Black denotes the daily number of earthquakes in the final TVZ catalogue and red shows cumulative number of earthquakes through time.

associate phase picks to a possible earthquake origin, *PyOcto* requires a one-dimensional velocity model. For our study, we employ the velocity model of Messtel (2023), which was developed for the Taupō region. While this study is focused on the TVZ, there were many earthquakes that occurred outside of the TVZ during our study period. Therefore, we used a search region for *PyOcto* that is much wider than the TVZ (Longitude: 173° to 178.5°, Latitude: -42° to -37°, Depth: -2 to 300 km). We found that using this wider search region stopped *PyOcto* from ‘mis-associating’ distant earthquakes into the region of interest. When creating the velocity grid, we allowed for a velocity model tolerance of two seconds. For the association stage we set a time slice overlap (`time_before`) of 300 seconds to account for the relatively large study area. We set the minimum number of picks for an earthquake to 10, with a minimum of 5 and 2 *P* and *S* picks, respectively. Finally,

we set the minimum grid node size (`min_node_size`) to 10 km, the number of times to subdivide the initial volume (`location_split_depth`) to 10, and the `location_split_return` value, which determines the size of the new search volume, to 5.

The association resulted in 288,229 individual earthquakes from a total of  $5.8 \times 10^6$  individual phases (17% of the input phases). These earthquakes were initially located by *PyOcto* using the 1D model. Before the next stage of earthquake catalogue generation, these earthquakes were then filtered to preserve only those that were in our area of interest (Longitude: 175° to 178°, Latitude: -40° to -37°, Depth: <50 km), meaning that 151,042 earthquakes progressed to the next stage.

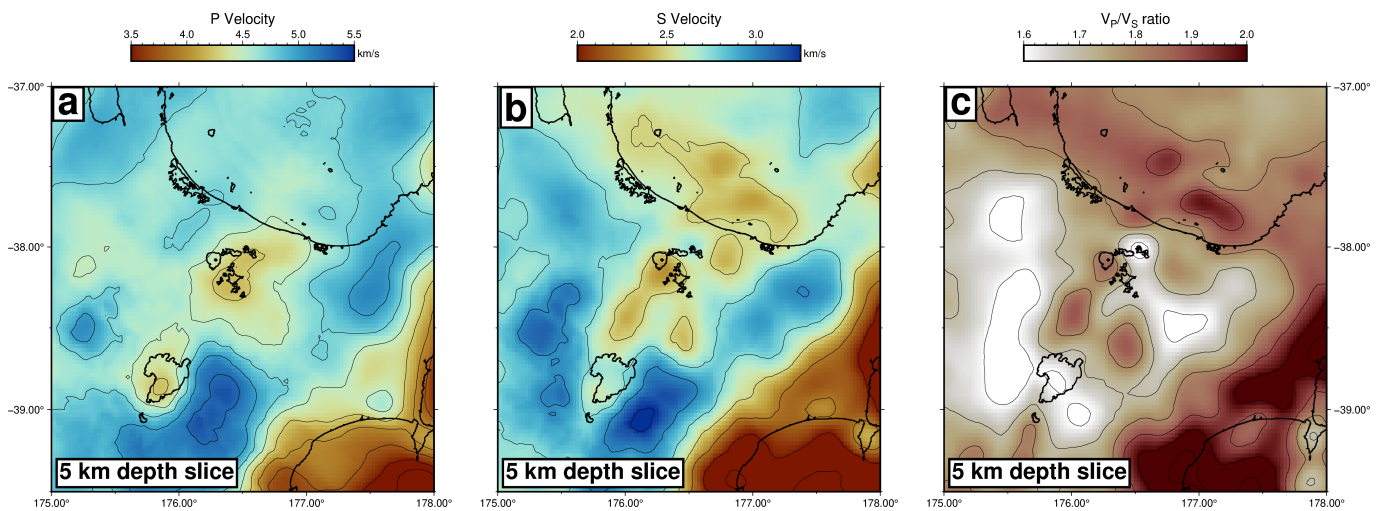


**Figure 3** 5 km depth slice through the velocity model of [Chow et al. \(2022\)](#) that we used in our study for earthquake location. a) P-wave velocity, b) S-wave velocity, c)  $V_P/V_S$  ratio.

## 2.4 Earthquake locating and magnitudes

*PyOcto* performs a relatively crude estimate of earthquake location. To improve this, we again locate the earthquake catalogue using *NonLinLoc* ([Lomax et al., 2000](#)) and a more representative velocity model. The TVZ is a highly complex and heterogeneous geological region; therefore a three-dimensional seismic velocity model will best capture the spatial variation in seismic properties. For our study, we used the three-dimensional velocity model for the North Island of New Zealand from [Chow et al. \(2022\)](#) (Figure 3). [Chow et al. \(2022\)](#) used earthquake adjoint tomography to image the shallow crust in the North Island. Their model is particularly sensitive to velocity variations in the upper 30 km of the crust and is therefore ideally suited for our study. Generally, both *P*- and *S*-wave velocities tend to be relatively slow in the TVZ, though there are local variations (Figure 3). For our earthquake location, we used a velocity model grid spacing of 1 km.

To produce absolute locations for our earthquake catalogue, we used *NonLinLoc* ([Lomax et al., 2000](#)) with the time-weighted Equal-Differential Time likelihood function ([Font et al., 2004](#)) and the Oct-Tree sampling algorithm ([Lomax and Curtis, 2001](#)). We used an assumed pick error of 0.3 seconds and included seismometer elevations in the location procedure. For the grid search, we applied a minimum cell size of 0.05 km and a maximum of  $1 \times 10^6$  iterations with an initial  $12 \times 12 \times 4$  Oct-Tree grid. We then applied a series of location quality filters to ensure that our final absolute location catalogue only contained well-constrained earthquakes. Each earthquake had to fulfill the following criteria: a maximum horizontal error  $< 5$  km; either an azimuthal gap  $< 180^\circ$  or a distance to the nearest seismometer of  $< 20$  km; a minimum of eight phase arrivals used for the location; and a maximum mean arrival time residual of 0.5 seconds. These quality filters were selected based on an iterative process which sought to remove earthquakes which were far outside of the TVZ network, remove any remaining falsely

associated earthquakes which had been mis-located inside the network, and retain all well-constrained TVZ earthquakes. This resulted in a total of 86,579 earthquakes, 57% of the earthquakes which were associated by *PyOcto*. The occurrence and location accuracy of these earthquakes have large spatial variations (Figure 4). Generally, earthquakes offshore of the Bay of Plenty tend to have larger location errors due to a lower number of phases; this is not surprising, given the relative reduction in network density in this region. In the on-land component of the TVZ, earthquake location errors and residuals are consistently low (Figure 4).

We then calculated local magnitudes ( $M_L$ ) for the entire catalogue. We first convolved the seismograms with the Wood-Anderson standard response ([Anderson and Wood, 1925](#); [Richter, 1935](#)), and then measured half the peak-to-peak displacement amplitude on the vertical component. These values were then used with the local magnitude scale from [Mestel \(2023\)](#) to calculate local magnitudes while accounting for attenuation ([Keir et al., 2006](#); [Illsley-Kemp et al., 2017](#)). Local magnitudes are appropriate for the majority of the earthquake catalogue; however, the magnitude will tend to be underestimated ([Hudson et al., 2022](#); [Illsley-Kemp et al., 2022](#)) for the small number of larger magnitude ( $> 4$ ) earthquakes. For the entire catalogue, local magnitudes range from  $-1.2$ – $4.5$  and the magnitude of completeness, calculated using the methodology of [Wiemer and Wyss \(2000\)](#), is 1.2, though this will vary with both space and time.

The final stage of our earthquake catalogue generation was to create a subset of earthquakes that are relocated using high-precision cross-correlation derived picks. These picks were then used in the well-established relative-relocation procedure (e.g., [Waldhauser and Ellsworth, 2000](#); [Trugman and Shearer, 2017](#)). To generate differential travel-times, we cross-correlated waveforms for all earthquakes within a 10 km hypocentral distance of each other, using the *EQcorrscan* package ([Chamberlain et al., 2018](#)). We

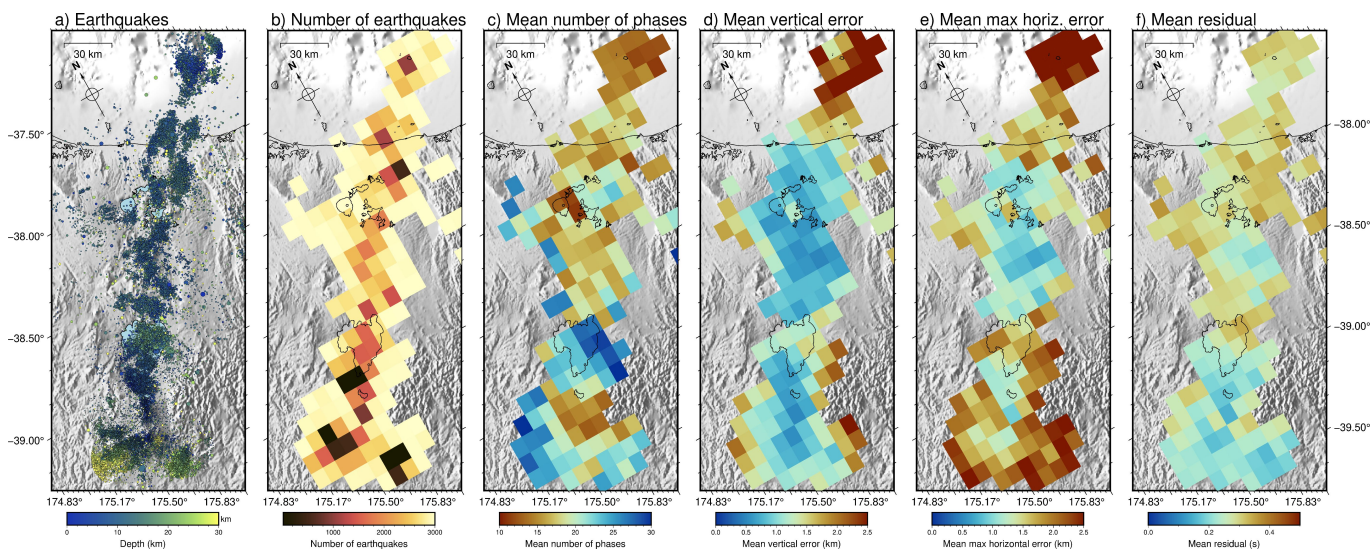


**Figure 4** a) All 86,579 earthquakes between 2007–2023 in the absolute location catalogue, coloured by depth. b) The number of earthquakes in  $0.1^\circ \times 0.1^\circ$  sub-regions which have  $>20$  earthquakes, plots c–f are divided into the same sub-regions. c) The mean number of phases used to locate earthquakes in each sub-region. d) The mean vertical error for all earthquakes in each sub-region. e) The mean maximum horizontal error for all earthquakes in each sub-region. f) The mean arrival time residual for all earthquakes in each sub-region.

detrended and filtered the seismic data between 1–15 Hz and used a correlation window 1 second wide, starting 0.3 seconds before the pick. To ensure only high-quality measurements, we only retained values with correlation  $>0.65$  and event pairs with more than 8 measurements, following Trugman (2024). This resulted in  $2.2 \times 10^8$  differential time measurements across  $1.7 \times 10^7$  event pairs.

For the relocation procedure, we used *GrowClust3D* (Trugman et al., 2023), a Julia implementation of the *GrowClust* algorithm (Trugman and Shearer, 2017) which allows for three-dimensional velocity models. We used the same velocity model as we used for the absolute location stage (Chow et al., 2022). We allowed clusters to merge if they were within a distance of 8 km and for these clusters to shift their locations by up to 2 km. This resulted in 55,969 (65%) of the input events being relocated, with a mean RMS differential time residual of 0.08 and 0.18 for *P* and *S* phases, respectively.

### 3 The TVZ earthquake catalogue

The final TVZ earthquake catalogue contains a huge amount of information, which we will not discuss in full detail here. Our hope is that by presenting and describing the catalogue here we will allow future detailed analysis and interpretation, as well as support other investigations that rely upon an understanding of seismic activity. The catalogue shows that earthquake activity in the TVZ is highly variable in time and tends to occur in geographically isolated swarms (Figure 5). Some of these swarms have previously been studied in detail, such as the activity at Taupō in 2019 (Illsley-Kemp et al., 2021) and 2022–23 (Lamb et al., 2024), but we also find many that require further investigation. To name a few, we find a remarkably persistent

earthquake swarm near the town of Waiouru, a distinct swarm near Matata that persists for the first six years of our catalogue, and intense earthquake activity to the southwest of Lake Taupō in 2008–2010, 2015 and 2017 (Figure 5).

The depth of earthquakes varies quite significantly along the length of the TVZ. At the southern end of the TVZ, seismicity spans almost the entire thickness of the crust (0–30 km), and is particularly deep to the west of Ruapehu (Figure 6). Beneath the andesitic volcanoes Ruapehu and Tongariro, seismicity is relatively limited, and when it does occur it tends to be in the upper 10 km of the crust. This depth distribution is also shared by the seismic activity to the southwest of Lake Taupō. However, this depth distribution changes at Taupō volcano, where the majority of the earthquakes are in the mid-crust (8–20 km depth). This is consistent with previous studies of Taupō seismicity (Illsley-Kemp et al., 2021, 2022; Mestel, 2023; Lamb et al., 2024). In the region from Taupō to Ōkataina, earthquake depths are remarkably consistent at around 9 km depth.

### 4 Discussion

It is our hope that this earthquake catalogue can be used for many future studies in the TVZ. This could include studies on individual volcanoes, structural geology and tectonics, geothermal exploitation, and perhaps more that we have not envisaged. We have therefore tried to make the data accessible to non-seismologists and here explain how to use the catalogue and some of its limitations. Firstly, a note on data format: in the Zenodo data repository, we present the catalogue in both QuakeML and CSV format. QuakeML is now a standard data format for earthquake catalogues and can be parsed with software such as *ObsPy* (Beyreuther

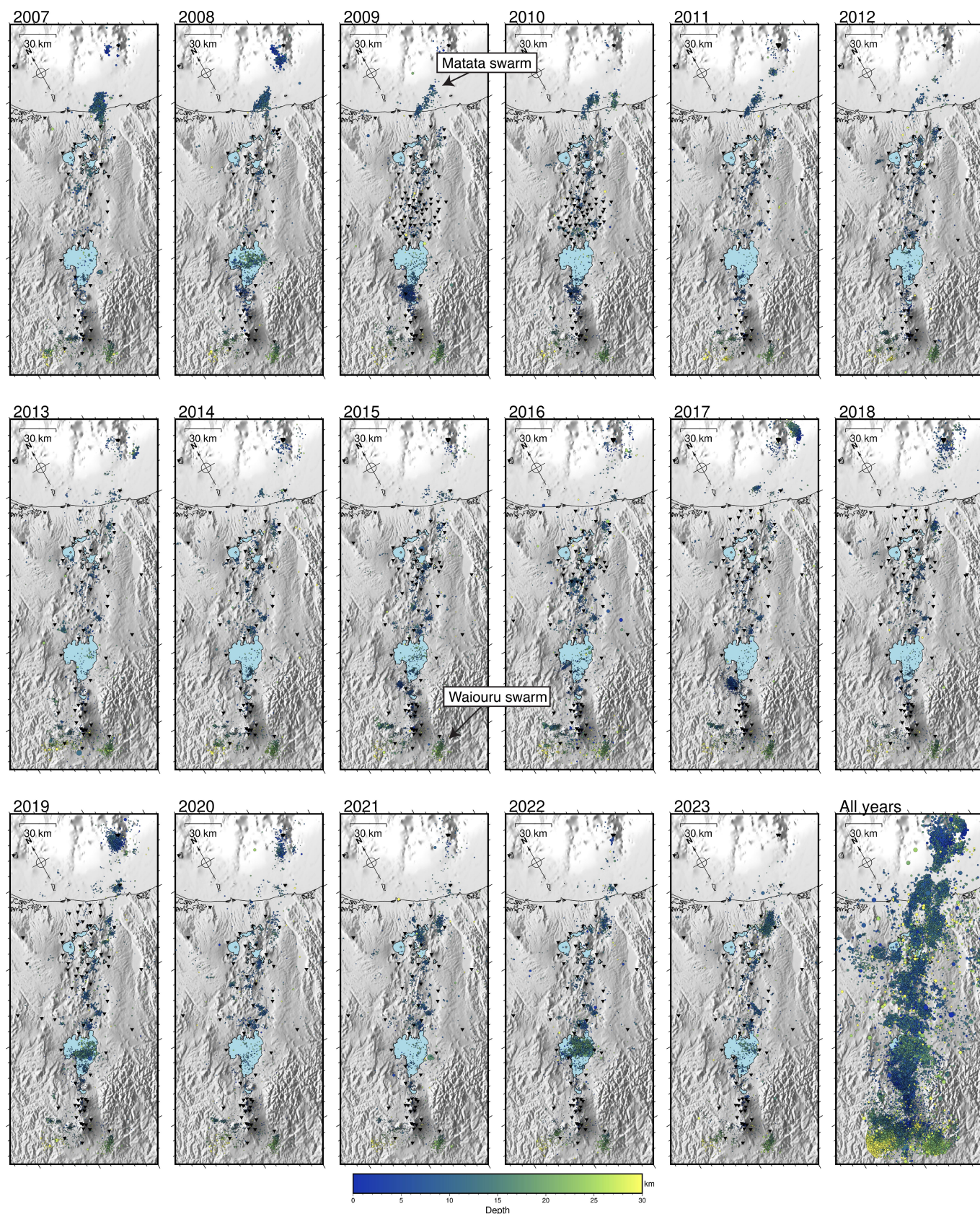


**Figure 5** Each panel shows the yearly breakdown of the absolute location earthquake catalogue, with each earthquake coloured by hypocentre depth. Swarms of note at Matata and Waiouru are labelled. The final panel shows the entire absolute location earthquake catalogue.

et al., 2010). It contains all of the earthquake metadata, including phase picks and amplitudes. Alongside this, we present the data in a simple CSV format which provides basic information about each earthquake such as

origin time, location, depth, and magnitude. The CSV format should be sufficient for most purposes, and can easily be converted into GIS-compatible formats.

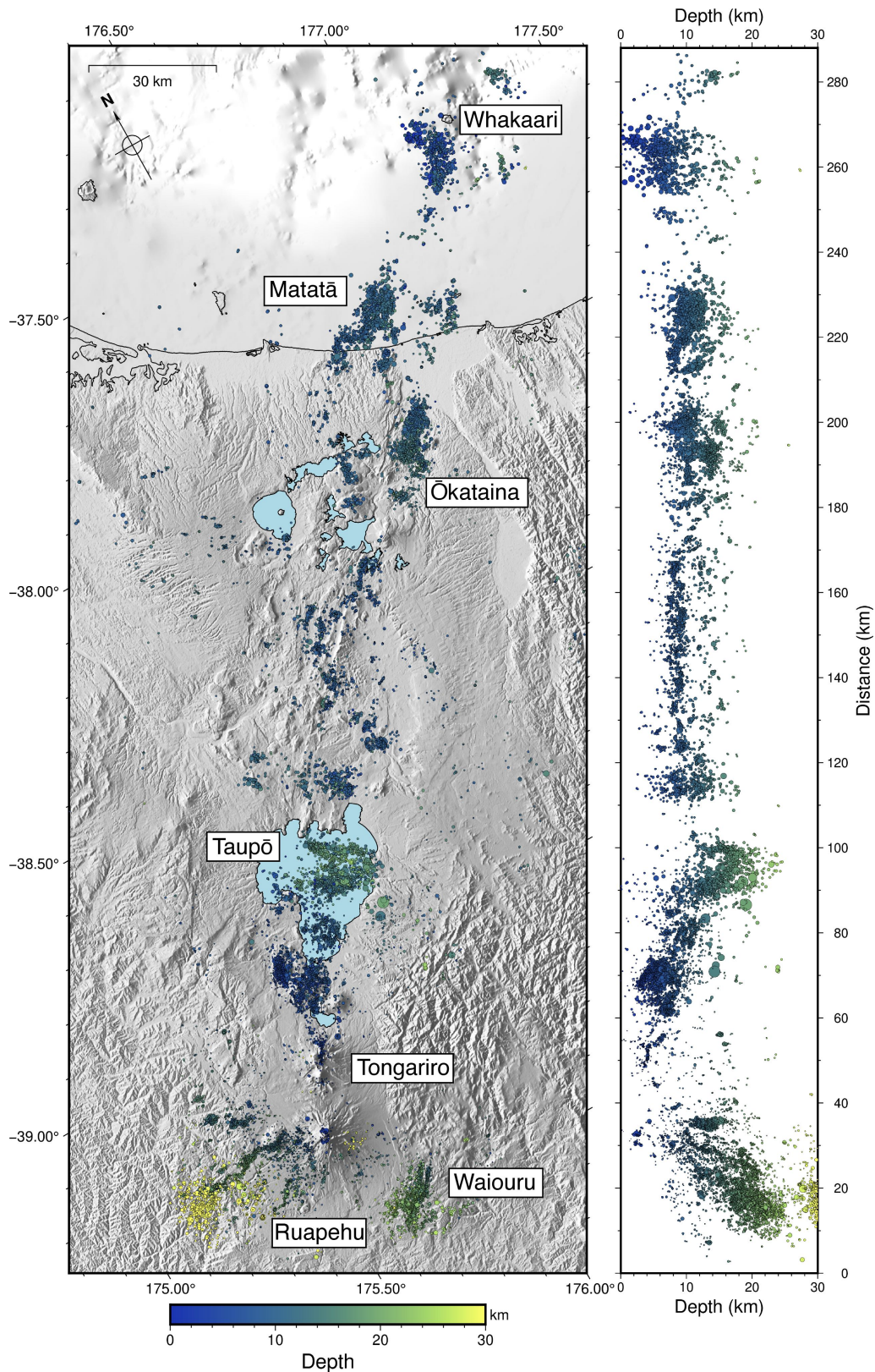


**Figure 6** The entire relocated earthquake catalogue, coloured by hypocentre depth. The right panel shows an along-TVZ cross section displaying the variation in earthquake depths along the TVZ.

The differences in location methodology, velocity model, magnitude calculation, and quality control procedure between our catalogue and the GeoNet catalogue (GNS Science, 2024) mean that it is not possible to meaningfully compare the errors in earthquake source parameters. However, we can make some basic comparisons of the two catalogues for the same time period

and approximate location. From 2007–2023, GeoNet detected 58,317 earthquakes in the TVZ (“Tongariro & Bay of Plenty” region), compared to the 86,579 earthquakes in the absolute earthquake catalogue presented here. The majority of these additional earthquakes are smaller-magnitude earthquakes not included in the GeoNet catalogue. The GeoNet catalogue for this region

has a magnitude of completeness of 2.0 and a minimum magnitude of -0.3. In comparison, the magnitude of completeness for our catalogue is 1.2 with a minimum magnitude of -1.2.

For any users of the catalogue, it is important to understand the distinction between the absolute earthquake locations (86,579 earthquakes, Figure 5) and the relocated earthquake locations (55,969 earthquakes, Figure 6). The relocated earthquake locations are useful for distinguishing fine-scale structures and earthquake migration through time. We illustrate the detail available from the relocated earthquakes in Figure 7, with an example from the Hipaua-Waihi-Tokaanu geothermal field. This geothermal field is expressed at the surface by hot springs, fumaroles, and the Hipaua Steaming Cliffs (Severne, 1999; Risk et al., 2002; Soto et al., 2019). However, there has been very little research into earthquake activity here. In the region shown in Figure 7, 12,254 earthquakes are detected in the absolute earthquake catalogue, 8,785 (72%) of which are relocated. The majority of these earthquakes occurred in distinct swarms in 2009–2010, 2015, and 2017 (Figure 5). The relocated earthquake catalogue illustrates that these earthquakes occur in discrete clusters at depths 3–7 km (Figure 7).

Due to the requirements of the relocation procedure, only 65% of earthquakes from the total catalogue were able to be relocated, and the analysis often excluded higher-magnitude earthquakes, which tend to have complex waveforms. This means that any studies that wish to investigate seismic moment release, seismic hazard, or changes in earthquake rates must use the entire earthquake catalogue, not just those that have been relocated.

#### 4.1 Limitations of the catalogue and future work

As with any earthquake catalogue, there are limitations to the one we present here and these should always be considered when using this data for future research. Firstly, the accuracy of any earthquake location relies upon the accuracy of the velocity model used in the location procedure. In our study, we used the three-dimensional model of Chow et al. (2022), which at the time of writing is the best available model for the North Island. However, this inevitably will not resolve fine-scale variations in seismic velocity at a local scale. Future studies that focus on a small geographic area may wish to locate the earthquakes in this catalogue with a local velocity model.

Users must also be careful with earthquakes that are at the edge of the seismic network. As with any earthquake catalogue, earthquakes that are outside of the seismic network have higher location uncertainties (Figure 4d, e). In addition, because we apply a quality criterion during our location procedure which requires that any earthquake be within 20 km of a seismometer, this produces artificial curves in the

earthquake distribution at the edge of the network; this is particularly apparent to the northeast of Whakaari and to the west of Ruapehu (Figure 5). Finally, the magnitudes presented here are local magnitudes, which are appropriate for the vast majority of the earthquakes but have been shown to underestimate magnitudes for earthquakes with magnitudes  $M_L > 4$  (Hudson et al., 2022; Illsley-Kemp et al., 2022). Future work could calculate moment magnitudes for these larger earthquakes. We also did not solve for or use individual station correction terms for this calculation. This could be a useful future addition, potentially combined with a three-dimensional inversion of attenuation.

By making the underlying phase picks available and documenting the full catalogue generation procedure, we make it straightforward to expand the earthquake catalogue as more seismic data becomes available, either through the passage of time or the lifting of data embargoes. This means that the value of this catalogue can increase with time, particularly when considering long-term trends in earthquake occurrence. We have also not performed any analyses of phase polarities or focal mechanisms. If appropriate methods can be developed to quickly and accurately produce polarity picks, this would be an excellent addition and would allow for detailed analyses of the stress field in the TVZ (e.g., Townend et al., 2012).

Finally, the *EQTransformer* model we use was trained on a global earthquake dataset that does not include low-frequency seismic events, which are known to occur in volcanic regions and have been documented in the TVZ (Hurst and Sherburn, 1993; Park et al., 2019; Steinke et al., 2024). This means that our earthquake catalogue will not include these earthquakes. Future work that seeks to detect and catalogue low-frequency seismicity (e.g., Zhong and Tan, 2024) would greatly improve our understanding of these signals in the TVZ, particularly alongside the earthquake catalogue presented here. It is also possible that the geological setting of the TVZ, in particular the high rates of seismic attenuation (Illsley-Kemp et al., 2022), may hinder the performance of the pre-trained model. Future work could train earthquake picking models on an earthquake dataset that is specifically designed for volcanic regions.

## 5 Conclusions

In this paper, we present a new consistent and high-precision earthquake catalogue for the Taupō Volcanic Zone, beginning in 2007 and covering the subsequent seventeen years to the end of 2023. The final earthquake catalogue contains 86,579 earthquakes, 65% of which were then further relatively relocated into a high-precision catalogue. The catalogue contains an enormous amount of information about volcanic and tectonic processes during this time period. We make the earthquake catalogue freely available to the scientific community in the hope that it will be used for further research and development.

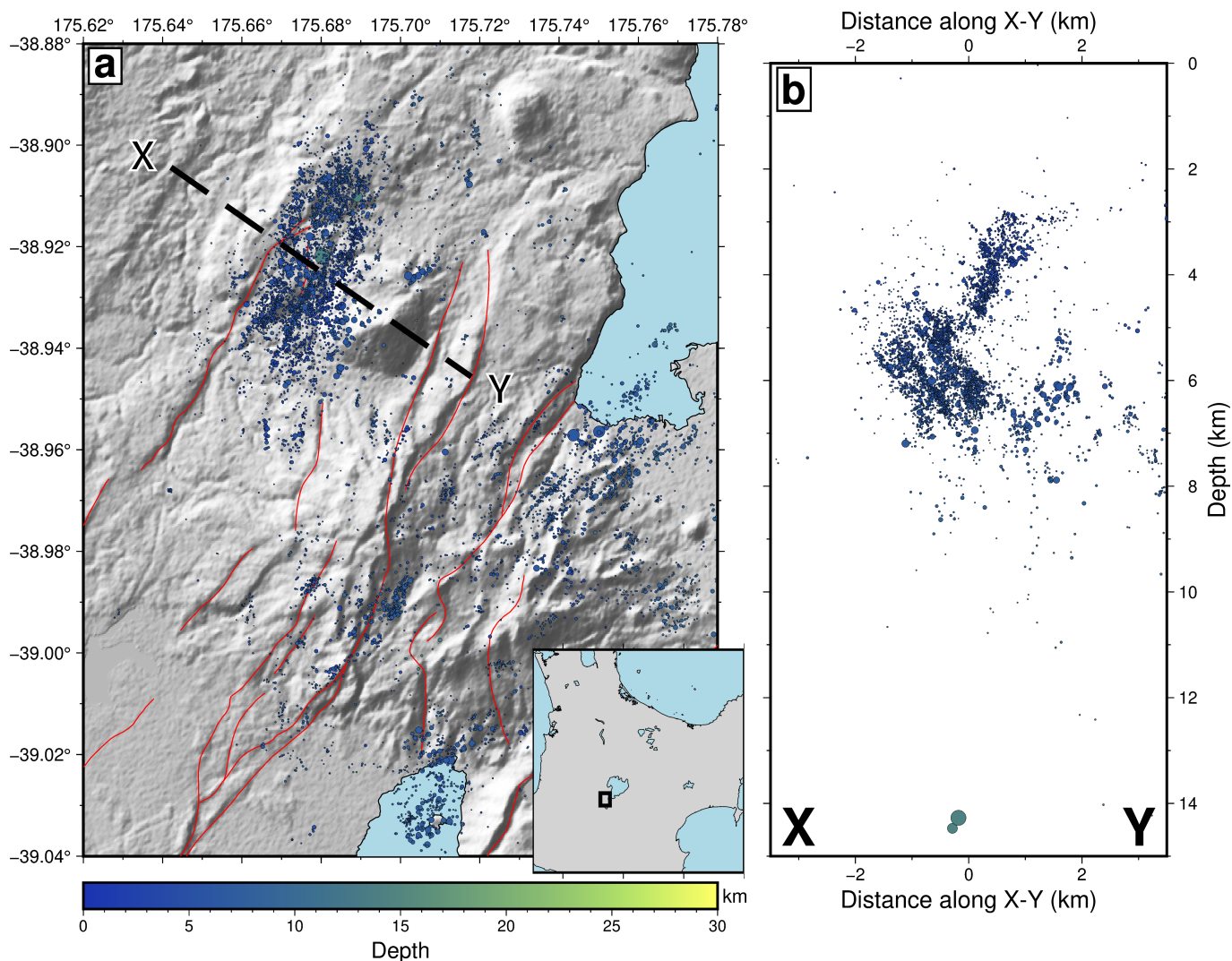


**Figure 7** A detailed look at the highly seismically active Hipaua-Waihi-Tokaanu geothermal field, southwest of Lake Taupō. The majority of earthquake activity here occurs in distinct swarms in 2009–2010, 2015, and 2017. This figure shows the relocated earthquake catalogue and highlights the level of detail that is present.

## Acknowledgements

FIK is supported by the Marsden Fund of the Royal Society of New Zealand (Grant MFP-VUW2109) and the Toka Tū Ake NHC Programme in Earthquake Seismology and Tectonic Geodesy at Victoria University of Wellington. Finally, we thank the editor, Lise Retailleau, and the two reviewers, Aude Lavayssière and Daniel Trugman, for their thoughtful comments.

## Data and code availability

The full earthquake catalogue is freely available at <https://doi.org/10.5281/zenodo.13138604>. The GeoNet seismic data is freely available through GeoNet (GNS Science, 2021). Figures were made with GMT6 (Wessel et al., 2019), Matplotlib (Hunter, 2007), and PyGMT (Tian et al., 2023).

## Competing interests

The authors have no competing interests.

## References

- Anderson, J. and Wood, H. O. Description and theory of the torsion seismometer. *Bulletin of the Seismological Society of America*, 15 (1):1–72, 1925. doi: <https://doi.org/10.1785/BSSA0150010001>.
- Bannister, S. Deep Geothermal HADES seismic array [Data set], 2009. doi: [https://doi.org/10.7914/SN/Z8\\_2009](https://doi.org/10.7914/SN/Z8_2009).
- Bannister, S., Sherburn, S., and Bourguignon, S. Earthquake swarm activity highlights crustal faulting associated with the Waimangu–Rotomahana–Mt Tarawera geothermal field, Taupo Volcanic Zone. *Journal of Volcanology and Geothermal Research*, 314:49–56, 2016. doi: <https://doi.org/10.1016/j.jvolgeores.2015.07.024>.
- Benson, T. W., Illsley-Kemp, F., Elms, H. C., Hamling, I. J., Savage, M. K., Wilson, C. J. N., Mestel, E. R. H., and Barker, S. J. Earthquake analysis suggests dyke intrusion in 2019 near Tarawera volcano, New Zealand. *Frontiers in Earth Science*, 8:606992, 2021. doi: <https://doi.org/10.3389/feart.2020.606992>.
- Beyreuther, M., Barsch, R., Krischer, L., Megies, T., Behr, Y., and Wassermann, J. ObsPy: A Python toolbox for seismology. *Seismological Research Letters*, 81(3):530–533, 2010. doi: <https://doi.org/10.1785/gssrl.81.3.530>.
- Bryan, C. J., Sherburn, S., Bibby, H. M., Bannister, S. C., and Hurst, A. W. Shallow seismicity of the central Taupo Volcanic Zone,

- New Zealand: Its distribution and nature. *New Zealand Journal of Geology and Geophysics*, 42(4):533–542, 1999. doi: <https://doi.org/10.1080/00288306.1999.9514859>.
- Chamberlain, C. J., Hopp, C. J., Boese, C. M., Warren-Smith, E., Chambers, D., Chu, S. X., Michailos, K., and Townend, J. EQ-corrscan: Repeating and near-repeating earthquake detection and analysis in python. *Seismological Research Letters*, 89(1): 173–181, 2018. doi: <https://doi.org/10.1785/0220170151>.
- Chow, B., Kaneko, Y., Tape, C., Modrak, R., Mortimer, N., Bannister, S., and Townend, J. Strong upper-plate heterogeneity at the Hikurangi subduction margin (North Island, New Zealand) imaged by adjoint tomography. *Journal of Geophysical Research: Solid Earth*, 127(1):e2021JB022865, 2022. doi: <https://doi.org/10.1029/2021JB022865>.
- Delano, J. E., Howell, A., Stahl, T. A., and Clark, K. 3D coseismic surface displacements from historical aerial photographs of the 1987 Edgecumbe earthquake, New Zealand. *Journal of Geophysical Research: Solid Earth*, 127(11):e2022JB024059, 2022. doi: <https://doi.org/10.1029/2022JB024059>.
- Ebinger, C. and Stern, T. Back-arc rifting in New Zealand [Data set], 2017. doi: [https://doi.org/10.7914/SN/YA\\_2017](https://doi.org/10.7914/SN/YA_2017).
- Font, Y., Kao, H., Lallemand, S., Liu, C.-S., and Chiao, L.-Y. Hypocentre determination offshore of eastern Taiwan using the maximum intersection method. *Geophysical Journal International*, 158:655–675, 2004. doi: <https://doi.org/10.1111/j.1365-246X.2004.02317.x>.
- GNS Science. GeoNet Aotearoa New Zealand Stations Metadata Repository [Dataset], 2019. <https://doi.org/10.21420/OVY2-C144>. doi: <https://doi.org/10.21420/OVY2-C144>.
- GNS Science. GeoNet Aotearoa New Zealand Seismic Digital Waveform Dataset [Dataset], 2021. doi: <https://doi.org/10.21420/G19Y-9D40>.
- GNS Science. GeoNet Aotearoa New Zealand Earthquake Catalogue [Dataset], 2024. doi: <https://doi.org/10.21420/OS8P-TZ38>.
- Hayes, G., Reyners, M., and Stuart, G. The Waiouru, New Zealand, earthquake swarm: Persistent mid crustal activity near an active volcano. *Geophysical Research Letters*, 31(19):L19613, 2004. doi: <https://doi.org/10.1029/2004GL020709>.
- Hopp, C., Sewell, S., Mroczek, S., Savage, M., and Townend, J. Seismic response to injection well stimulation in a high-temperature, high-permeability reservoir. *Geochemistry, Geophysics, Geosystems*, 20(6):2848–2871, 2019. doi: <https://doi.org/10.1029/2019GC008243>.
- Hudson, T. S., Kendall, J.-M., Pritchard, M. E., Blundy, J. D., and Gottsmann, J. H. From slab to surface: Earthquake evidence for fluid migration at Uturuncu volcano, Bolivia. *Earth and Planetary Science Letters*, 577:117268, 2022. doi: <https://doi.org/10.1016/j.epsl.2021.117268>.
- Hunter, J. D. Matplotlib: A 2D graphics environment. *Computing in Science & Engineering*, 9(3):90–95, 2007. doi: <https://doi.org/10.1109/MCSE.2007.55>.
- Hurst, A. W. and Sherburn, S. Volcanic tremor at Ruapehu: characteristics and implications for the resonant source. *New Zealand Journal of Geology and Geophysics*, 36(4):475–485, 1993. doi: <https://doi.org/10.1080/00288306.1993.9514593>.
- Hurst, T., Bannister, S., Robinson, R., and Scott, B. Characteristics of three recent earthquake sequences in the Taupo Volcanic Zone, New Zealand. *Tectonophysics*, 452(1-4):17–28, 2008. doi: <https://doi.org/10.1016/j.tecto.2008.01.017>.
- Illsley-Kemp, F., Keir, D., Bull, J. M., Ayele, A., Hammond, J. O., Kendall, J.-M., Gallacher, R. J., Gernon, T., and Goitom, B. Local earthquake magnitude scale and b-value for the Danakil region of northern Afar. *Bulletin of the Seismological Society of America*, 107(2):521–531, 2017. doi: <https://doi.org/10.1785/0120150253>.
- Illsley-Kemp, F., Barker, S. J., Wilson, C. J. N., Chamberlain, C. J., Hreinsdóttir, S., Ellis, S., Hamling, I. J., Savage, M. K., Mestel, E. R. H., and Wadsworth, F. B. Volcanic unrest at Taupō volcano in 2019: Causes, mechanisms and implications. *Geochemistry, Geophysics, Geosystems*, 22:e2021GC009803, 2021. doi: <https://doi.org/10.1029/2021GC009803>.
- Illsley-Kemp, F., Herath, P., Chamberlain, C. J., Michailos, K., and Wilson, C. J. N. A decade of earthquake activity at Taupō Volcano, New Zealand. *Volcanica*, 5(2):335–348, 2022. doi: <https://doi.org/10.30909/vol.05.02.335348>.
- Keir, D., Stuart, G., Jackson, A., and Ayele, A. Local earthquake magnitude scale and seismicity rate for the Ethiopian Rift. *Bulletin of the Seismological Society of America*, 96(6):2221–2230, 2006. doi: <https://doi.org/10.1785/0120060051>.
- Lamb, O., Bannister, S., Ristau, J., Miller, C., Sherburn, S., Jacobs, K., Hanson, J., D’Anastasio, E., Hreinsdóttir, S., Snee, E., et al. Seismic characteristics of the 2022–2023 unrest episode at Taupō volcano, Aotearoa New Zealand. *Seismica*, 3(2), 2024. doi: <https://doi.org/10.26443/seismica.v3i2.1125>.
- Lomax, A. and Curtis, A. Fast, probabilistic earthquake location in 3D models using oct-tree importance sampling. In *Geophysical Research Abstracts*, volume 3, pages 10–1007, 2001.
- Lomax, A., Virieux, J., Volant, P., and Berge-Thierry, C. Probabilistic earthquake location in 3D and layered models. *Modern Approaches in Geophysics*, 18:101–134, 2000. doi: [https://doi.org/10.1007/978-94-015-9536-0\\_5](https://doi.org/10.1007/978-94-015-9536-0_5).
- Mark, O. K., Illsley-Kemp, F., Townend, J., and Barker, S. J. Evidence From intermediate-depth earthquakes of slab-derived fluids beneath the Taupō Volcanic Zone. *Journal of Geophysical Research: Solid Earth*, 129(5):e2023JB028586, 2024. doi: <https://doi.org/10.1029/2023JB028586>.
- Mestel, E. R. H. *Seismicity, sub-surface structure and partnership with Tangata Whenua of Taupō volcano*. PhD thesis, Te Herenga Waka Victoria University of Wellington, 2023. doi: <https://doi.org/10.26686/wgtn.24405691>.
- Mousavi, S. M., Sheng, Y., Zhu, W., and Beroza, G. C. STanford Earthquake Dataset (STEAD): A global data set of seismic signals for AI. *IEEE Access*, 7:179464–179476, 2019. doi: <https://doi.org/10.1109/access.2019.2947848>.
- Mousavi, S. M., Ellsworth, W. L., Zhu, W., Chuang, L. Y., and Beroza, G. C. Earthquake transformer—an attentive deep-learning model for simultaneous earthquake detection and phase picking. *Nature Communications*, 11(1):3952, 2020. doi: <https://doi.org/10.1038/s41467-020-17591-w>.
- Münchmeyer, J. PyOcto: A high-throughput seismic phase associator. *Seismica*, 3(1), 2024. doi: <https://doi.org/10.26443/seismica.v3i1.1130>.
- Park, I., Jolly, A., Kim, K. Y., and Kennedy, B. Temporal variations of repeating low frequency volcanic earthquakes at Ngauruhoe Volcano, New Zealand. *Journal of Volcanology and Geothermal Research*, 373:108–119, 2019. doi: <https://doi.org/10.1016/j.jvolgeores.2019.01.024>.
- Petersen, T., Gledhill, K., Chadwick, M., Gale, N. H., and Ristau, J. The New Zealand national seismograph network. *Seismological Research Letters*, 82(1):9–20, 2011. doi: <https://doi.org/10.1785/gssrl.82.1.9>.
- Pita-Sllim, O., Chamberlain, C. J., Townend, J., and Warren-Smith, E. Parametric testing of EQTransformer’s performance against a high-quality, manually picked catalog for reliable and accurate seismic phase picking. *The Seismic Record*, 3(4):332–341, 2023. doi: <https://doi.org/10.1785/0320230024>.

- Richter, C. An instrumental earthquake magnitude scale. *Bulletin of the Seismological Society of America*, 25(1):1–32, 1935. doi: <https://doi.org/10.1785/BSSA0250010001>.
- Risk, G. F., Bibby, H. M., Bromley, C. J., Caldwell, T. G., and Bennie, S. L. Appraisal of the Tokaanu–Waihi geothermal field and its relationship with the Tongariro geothermal field, New Zealand. *Geothermics*, 31(1):45–68, 2002. doi: [https://doi.org/10.1016/S0375-6505\(01\)00017-7](https://doi.org/10.1016/S0375-6505(01)00017-7).
- Seebeck, H., Nicol, A., Villamor, P., Ristau, J., and Pettinga, J. Structure and kinematics of the Taupo Rift, New Zealand. *Tectonics*, 33(6):1178–1199, 2014. doi: <https://doi.org/10.1002/2014TC003569>.
- Severne, C. M. *The Tokaanu–Waihi Geothermal System*. PhD thesis, University of Auckland, 1999.
- Sherburn, S. The 1987 January Tokaanu earthquake sequence, New Zealand. *New Zealand Journal of Geology and Geophysics*, 36(1):61–68, 1993. doi: <https://doi.org/10.1080/00288306.1993.9514554>.
- Sherburn, S., Bryan, C. J., Hurst, A. W., Latter, J. H., and Scott, B. J. Seismicity of Ruapehu volcano, New Zealand, 1971–1996: a review. *Journal of Volcanology and Geothermal Research*, 88(4):255–278, 1999. doi: [https://doi.org/10.1016/S0377-0273\(99\)00014-1](https://doi.org/10.1016/S0377-0273(99)00014-1).
- Smith, E. G. C. and Oppenheimer, C. M. M. The Edgecumbe earthquake sequence: 1987 February 21 to March 18. *New Zealand Journal of Geology and Geophysics*, 32(1):31–42, 1989. doi: <https://doi.org/10.1080/00288306.1989.10421386>.
- Soto, M. F., Hochstein, M. P., Campbell, K., and Keys, H. Sporadic and waning hot spring activity in the Tokaanu Domain, Hipaua–Waihi–Tokaanu geothermal field, Taupo Volcanic Zone, New Zealand. *Geothermics*, 77:288–303, 2019. doi: <https://doi.org/10.1016/j.geothermics.2018.10.005>.
- Steinke, B., Jolly, A. D., Girona, T., Caudron, C., Bramwell, L., Cronin, S. J., Illsley-Kemp, F., and Hughes, E. C. Dynamics and Detection of Pulsed Tremor at Whakaari (White Island), Aotearoa New Zealand. *Geophysical Research Letters*, 2024. doi: <https://doi.org/10.1029/2024GL110447>.
- Tian, D., Uieda, L., Leong, W. J., Schlitzer, W., Fröhlich, Y., Grund, M., Jones, M., Toney, L., Yao, J., Magen, Y., Tong, J.-H., Materna, K., Belem, A., Newton, T., Anant, A., Ziebarth, M., Quinn, J., and Wessel, P. PyGMT: A Python interface for the Generic Mapping Tools. doi: <https://doi.org/10.5281/zenodo.8303186>.
- Townend, J., Sherburn, S., Arnold, R., Boese, C., and Woods, L. Three-dimensional variations in present-day tectonic stress along the Australia–Pacific plate boundary in New Zealand. *Earth and Planetary Science Letters*, 353–354:47–59, 2012. doi: <https://doi.org/10.1016/j.epsl.2012.08.003>.
- Trugman, D. T. A High-Precision Earthquake Catalog for Nevada. *Seismological Research Letters*, 95(6):3737–3745, 06 2024. doi: <http://doi.org/10.1785/0220240106>.
- Trugman, D. T. and Shearer, P. M. GrowClust: A hierarchical clustering algorithm for relative earthquake relocation, with application to the Spanish Springs and Sheldon, Nevada, earthquake sequences. *Seismological Research Letters*, 88(2A):379–391, 2017. doi: <https://doi.org/10.1785/0220160188>.
- Trugman, D. T., Chamberlain, C. J., Savvaidis, A., and Lomax, A. GrowClust3D.jl: A Julia package for the relative relocation of earthquake hypocenters using 3D velocity models. *Seismological Society of America*, 94(1):443–456, 2023. doi: <https://doi.org/10.1785/0220220193>.
- Waldhauser, F. and Ellsworth, W. L. A double-difference earthquake location algorithm: Method and application to the northern Hayward fault, California. *Bulletin of the Seismological Society of America*, 90(6):1353–1368, 2000. doi: <https://doi.org/10.1785/0120000006>.
- Webb, T. H., Ferris, B. G., and Harris, J. S. The Lake Taupo, New Zealand, earthquake swarms of 1983. *New Zealand Journal of Geology and Geophysics*, 29(4):377–389, 1986. doi: <https://doi.org/10.1080/00288306.1986.10422160>.
- Wessel, P., Luis, J. F., Uieda, L., Scharroo, R., Wobbe, F., Smith, W. H. F., and Tian, D. The generic mapping tools version 6. *Geochemistry, Geophysics, Geosystems*, 20(11):5556–5564, 2019. doi: <https://doi.org/10.1029/2019GC008515>.
- Wiemer, S. and Wyss, M. Minimum magnitude of completeness in earthquake catalogs: Examples from Alaska, the western United States, and Japan. *Bulletin of the Seismological Society of America*, 90(4):859–869, 2000. doi: <https://doi.org/10.1785/0119990114>.
- Wilson, C. J. N., Houghton, B. F., McWilliams, M. O., Lanphere, M. A., Weaver, S. D., and Briggs, R. M. Volcanic and structural evolution of Taupo Volcanic Zone, New Zealand: A review. *Journal of Volcanology and Geothermal Research*, 68(1-3):1–28, 1995. doi: [https://doi.org/10.1016/0377-0273\(95\)00006-G](https://doi.org/10.1016/0377-0273(95)00006-G).
- Wilson, C. J. N., Gravelly, D. M., Leonard, G. S., and Rowland, J. V. Volcanism in the central Taupo Volcanic Zone, New Zealand: Tempo, styles and controls. *Studies in volcanology: the legacy of George Walker. Special Publications of IAVCEI*, 2:225–247, 2009. doi: <https://doi.org/10.1144/iavcel002.12>.
- Woollam, J., Münchmeyer, J., Tilmann, F., Rietbrock, A., Lange, D., Bornstein, T., Diehl, T., Giunchi, C., Haslinger, F., Jozinović, D., et al. SeisBench—A toolbox for machine learning in seismology. *Seismological Society of America*, 93(3):1695–1709, 2022. doi: <https://doi.org/10.1785/0220210324>.
- Zhong, Y. and Tan, Y. J. Deep-learning-based phase picking for volcano-tectonic and long-period earthquakes. *Geophysical Research Letters*, 51(12):e2024GL108438, 2024. doi: <https://doi.org/10.1029/2024GL108438>.

The article *A new consistent and high-precision earthquake catalogue for the Taupō Volcanic Zone, New Zealand* © 2025 by Finnigan Illsley-Kemp is licensed under CC BY 4.0.